Microstructure Investigation of Small-Section Nodular Iron Castings with Chunky Graphite

Iker Asenjo[1,a], Jacques Lacaze[2,b], Peio Larrañaga[1,c], Susana Méndez[1,d], Jon Sertucha[1,e], Ramón Suárez[1,f]

[1]Engineering and Foundry Processes Department, AZTERLAN, Aliendalde Auzunea 6, E-48200 Durango (Bizkaia), Spain

[2]CIRIMAT, Université de Toulouse, ENSIACET, BP 74233, 31432 Toulouse cedex 4, France

[a]iasenjo@azterlan.es, [b]jacques.lacaze@ensiacet.fr, [c]plarranaga@azterlan.es, [d]smendez@azterlan.es, [e]jsertucha@azterlan.es, [f]rsuarez@azterlan.es

Keywords: nodular iron, chunky graphite, light-section castings

Abstract. Parameters that affect chunky graphite formation in heavy-section castings have been studied in previous works which showed that inoculation and cerium addition both increase the tendency for this degenerate graphite. This suggested that laboratory study on chunky graphite formation could be performed on small castings by over-treating the melt. Though the role of silicon was not ascertained, it appeared of potential interest to also investigate its effect in relation with the carbon equivalent of the iron and the nucleation potential of the melt. Keel-blocks were thus cast using Ce or Ce-Mg treated melts, with increased silicon content (up to 4.0 wt.%) and inoculation rate as compared to usual practice. It was observed that chunky graphite systematically appeared in more or less extended areas centred on the upper part of the keel-blocks. The as-cast microstructure (graphite shape and distribution) has then been studied in relation to melt composition and additions (Ce treatment and inoculation) in both affected and non-affected areas. Finally, microanalysis of oxides and other minor phases showed them to be similar to those appearing in heavy-section castings. It may then be concluded that chunky graphite appears in light-section castings in the same way than in heavy-section castings when using over-treated melts.

Introduction

The formation of chunky graphite (CHG) has generally been related to the thermal centre of heavy-section ductile iron castings [1-5], though it may also appear in light-section castings [5] and is often reported in Ni-bearing cast irons [6]. Previously, large blocks have been used to determine those factors that affect CHG appearance in heavy-section ductile iron castings. It has been established that CHG is promoted by: i) high Si contents and over post-inoculation [7]; ii) additions of Ce normally associated with the use of Mg-master alloys [8, 9] and iii) long solidification times [7]. These results suggested enhancing the two first critical factors in order to promote CHG appearance in light size castings where solidification rates are usually large enough for avoiding graphite degeneration. Standard keel-blocks were thus cast using usual processing parameters but with various amounts of inoculant, of Si and of Ce. Microstructure analysis and microanalyses were then carried out for comparing CHG formation in keel-blocks with that in heavy-section castings.

Experimental Procedure

The test castings used in the present study are keel-blocks of type II (UNE-EN 1563) cast in chemical bonded sand moulds. Each mould contained three keel-block cavities. Melts were prepared in a 100 kg capacity medium frequency furnace (250 Hz) with metallic charges consisting of 50% pig iron and 50% returns from heavy section ductile iron castings. The C and Si contents were appropriately varied by addition of pure graphite (98%) and FeSi75 (75.1 Si, 0.31 Ca, 0.83 Al, 0.013 P, 0.001 S, wt.%) respectively, in order to get hypo, hyper and nearly eutectic alloys. Spheroidisation treatment was carried out using a 50 kg capacity ladle by addition of Ce-rich misch-

metal (CeMM: 67.0 Ce, 33.0 La, 0.25 Fe, wt.%) and/or FeSiMg (43.5 Si, 5.96 Mg, 0.95 Ca, 0.48 Al, 1.08 RE, wt.%) to the melt using the sandwich method. Inoculation was performed by adding 0.45% of the melt weight of a commercial inoculant (70-78 Si, 3.2-4.5 Al, 0.3-1.5 Ca and ~0.5 RE, wt.%) as inserts placed in the gating system before the ceramic filter. An extra addition (0.20 wt.%) of the same inoculant in powder (grain size 0.2 to 0.6 mm) was made at the bottom of one of the cavities while other additions could be similarly placed in the two other cavities.

After shaking out, the castings were transversely cut in the middle to obtain a 15 mm thick slice. In most cases the surface area of the section affected by CHG (C_C) could be directly measured as the darkened region that appears on the cut surface (Fig. 1-a), and was sometimes ascertained by metallographic observations. The local fraction of CHG (A_A) is zero outside the affected zone and takes a finite value inside this zone where it was evaluated following a procedure described previously [7]. Graphite particle counts (N_P) have been measured on five fields at an enlargement of 100x located in the CHG free zone considering only particles with area larger than 20 μm^2. A nodularity index NI was also evaluated as the ratio of the number of spheroidal particles to the total amount of graphite particles. The values of C_C, A_A, N_P and NI are given in Table 1.

Table 1. Casting reference, nodulizer additions, CHG evaluation (C_C and A_A), C, Si, carbon equivalent (CE), Ce and Mg content, graphite particles count (N_P) and nodularity index (NI).

Keel-block No.	Melt treatment (wt.% added)	C_C (%)	A_A (%)	C (wt.%)	Si (wt.%)	CE (wt.%)	Ce (ppm)	Mg (ppm)	N_P (mm^{-2})	NI (%)
#1	0.17 CeMM	72	65	3.24	3.68	4.27	640		110	85
			0	3.13	3.58	4.13	860			
#2	0.21 CeMM	45	60	3.62	2.49	4.32	740		60	85
			0	3.60	2.55	4.31	800			
#3	0.20 CeMM, 1.4 FeSiMg	10	10	3.47	2.71	4.23	750	374	90	90
#4*	0.28 CeMM	10	10	3.55	2.39	4.21	1180		50	50
#5	0.18 CeMM	80	65	3.58	2.63	4.32	500		300	90
			0	3.61	2.78	4.39	460			
#6	0.14 CeMM	24	40	3.51	2.83	4.30	540		175	70
			0	3.52	2.78	4.30	600			
#7	0.14 CeMM	29	30	3.76	2.76	4.53	660		160	80
			0	3.82	2.85	4.62	840			
#8	0.14 CeMM	20	30	3.43	2.97	4.26	440		225	80
			0	3.49	3.02	4.34	340			
#9	1.6 FeSiMg	0	0	3.50	2.92	4.32	51	290 Mg	200	85
#10	0.20 CeMM	15	10	3.48	2.77	4.26	270		175	30
#11	0.20 CeMM	85	100	3.24	2.57	3.96	647		80	70
#12	0.20 CeMM	85	100	3.16	2.94	3.98	586		125	75
#13	0.20 CeMM	80	80	3.57	2.62	4.30	594		150	85
#14	1.6 FeSiMg	0	0	3.58	2.73	4.34	47	242 Mg	250	90
#15**	1.6 FeSiMg	65	20	3.50	3.96	4.61	64	301 Mg	280	90

* Carbides. ** Graphite flotation.

Chemical analyses were carried out as indicated elsewhere [10] where the whole compositions are given. In Table 1, only the C, Si and Ce contents are listed as well as the Mg contents when this element was added. Also, the carbon equivalent CE (wt.%) calculated as CE=%C+0.28×%Si is given in Table 1. In many cases only a central sample was analyzed, but in some cases the chemical composition could be measured on two samples from the same keel-block: one with a high fraction of CHG (finite A_A value) and the other from the area of the keel-block that was not affected by

CHG (zero A_A value). The results of both analyses are differentiated in Table 1 in those cases. Samples were then machined out from the keel-blocks for metallographic analyses.

Microanalysis of inclusions was carried out for some of the keel-blocks using energy dispersive spectrometry (EDS) in a scanning electron microscope (SEM). This was done on fields 0.133 mm^2 in area for samples treated with CeMM and 0.042 mm^2 for samples treated with FeSiMg where the inclusions were more difficult to detect and a higher enlargement was necessary.

Results and Discussion

The micrographs in Fig. 1 show the microstructure observed in the hypo-eutectic #1 (Fig. 1b) and the hyper-eutectic #7 (Fig. 1c) castings. The bottom micrographs are from areas free from CHG, the top ones from areas with graphite degeneracy. In the affected area of the hypo-eutectic alloy, dendrites appear delineated by the CHG cells and very few graphite nodules can be observed. This shows that, as expected for a hypo-eutectic cast iron, solidification of this keel-block started with the development of a network of austenite dendrites. On the contrary, some nodules are detected in the area affected by CHG of the hyper-eutectic alloy which have a size similar to that of the largest nodules found in the CHG-free area of this keel-block. These nodules may thus be associated with primary graphite precipitation.

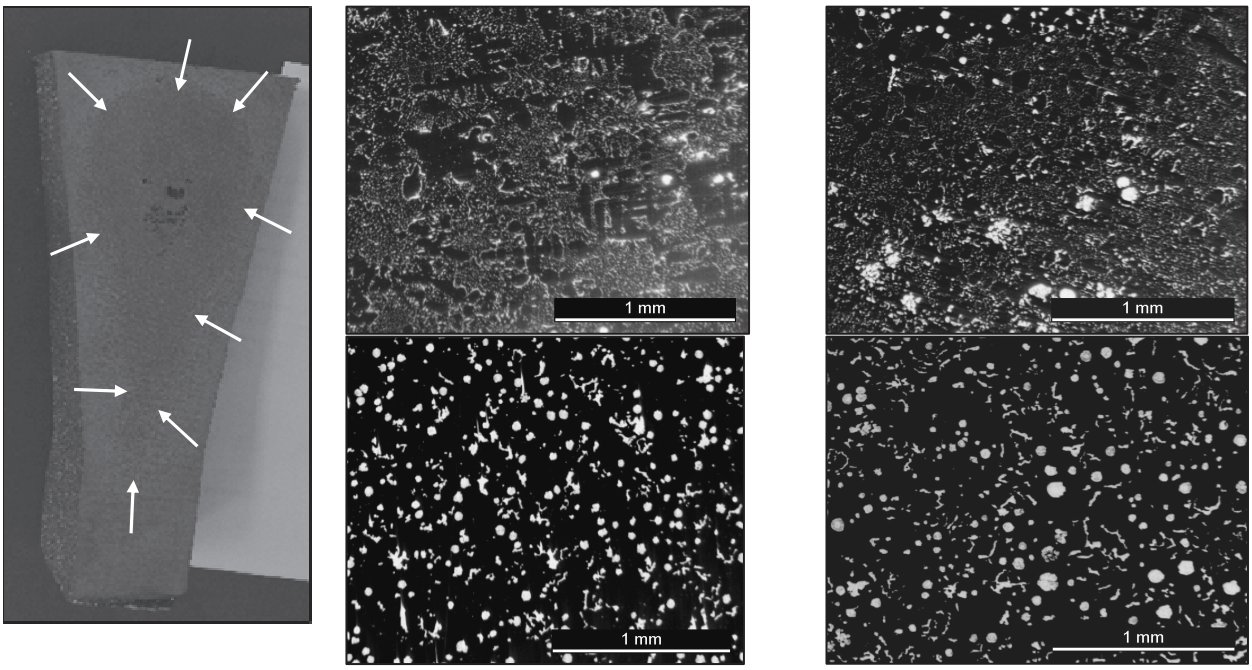

Fig. 1. Transverse cut of a keel-block with arrows pointing to the outer limit of the area affected by chunky graphite (a); micrographs of hypo-eutectic (b) and hyper-eutectic (c) alloys, from an area without chunky graphite (bottom row) or with such degenerate graphite (upper row).

In most of the castings of the present series, graphite precipitates do not appear to be fully spheroidal even in the CHG-free areas, as made apparent by the NI values in Table 1. It is seen that low nodularity is generally related to treatment with CeMM only, while the highest NI values are obtained using Mg or Ce-Mg treatment. The nodularizing effect of Ce is however ascertained by the observation that the lower its content the lower the NI values are. There are however two exceptions: i) trial #5 that achieves a high NI value with a medium level of CeMM addition; ii) trial #4 with the highest Ce addition that shows a low NI value. While the former exception seems to be an outlier, the latter is related to carbide precipitation. As reported previously for large blocks [9], it has been observed in keel-blocks that addition of Ce decreases the minimum eutectic temperature, and this was associated to a decrease in both graphite nucleation and growth. The effect on graphite nucleation is illustrated in Fig. 2 by the relation between Np and Ce content. The temperature decrease can be such that transition from stable to metastable (white) solidification may occur [10].

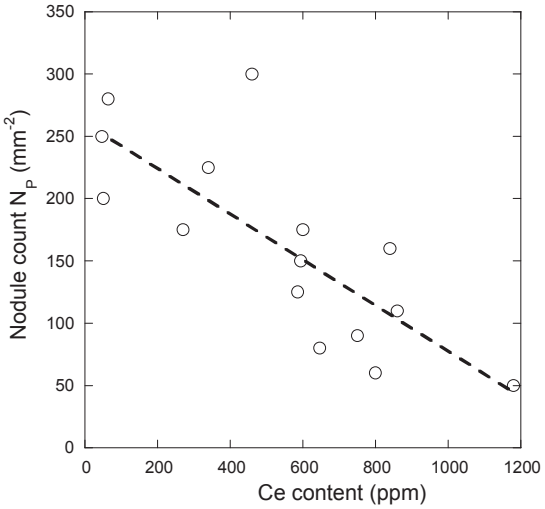

Fig. 2. Influence of the Ce content on N_P.

It was noticed also that when only Mg was used as spheroidizer (trials #9, #14 and #15) CHG only appeared in the keel-block with the highest Si content (trial #15). In this latter trial, the chunky cells were spread over the whole surface of the keel-block, so that the area affected (C_C) was quite large while the local fraction (A_A) was rather low. Although Mg-treated keel-block obtained in trial #3 also showed CHG, the appearance of this defect could be associated with the simultaneous addition of CeMM as spheroidizer. It may thus be concluded that Ce addition promotes CHG appearance under high cooling rates as it does at low cooling rates though no clear relation was found between the Ce content and C_C or A_A values.

Table 1 shows that the carbon equivalent of areas with CHG (finite A_A value) is generally closer to the eutectic value (CE=4.34 wt.%) than the area free of CHG (A_A=0). This is illustrated in Fig. 3 where the arrows show the shift in CE from the no-CHG to the CHG areas for the hypo-eutectic and hyper-eutectic alloys. The greyed area around the eutectic CE value corresponds to ±U, where U is the uncertainty on the CE value estimated at 0.06 wt.% [11] from the average carbon and silicon contents of the alloys used in the present study. This could possibly be due to graphite flotation in the case of the hypereutectic alloys. For the hypoeutectic alloy, one could relate it to the preferential formation and subsequent growth of austenite dendrites on the outer surface leading to a slightly higher fraction of eutectic in the centre of the casting. Such a phenomenon may be called a meso-segregation associated to microstructure development, it does indirectly confirm the eutectic nature of CHG cells.

Systematic observations of the samples to analyse inclusions were performed on four keel-blocks. In Fig. 4, CHG is seen at the bottom and graphite spheroids at the top of the micrograph. This area at the border of a CHG cell will be called a frontier area. Spot analysis was performed on inclusions and the number of each kind was evaluated, see Table 2. In this table, a few observations on heavy blocks from previous unpublished work (trials PW-1, PW-2 and PW-3) and from Källbom [12] have been included. In the samples treated with CeMM, most of the particles observed contain Ce, La and S, with sometimes a small contribution from the matrix seen through the Fe signal. According to the EDS analysis the most probable compound is (Ce,La)S. The second most numerous particles contain P and Ce, and the compound should be CeP. When CeP particles were analyzed, oxygen was also often observed together with a higher signal of Ce, leading to the suggestion that CeP particles could be associated with Ce oxide (Ce-O) precipitation. Although this latter particles were not counted, they are indicated in the last column of Table 2 when many of them could be noticed. In melts treated with FeSiMg in place of CeMM, the sulphur-bearing particles are MgS as expected, together with a small number of (Ce,La)S particles due to the RE elements contained in the FeSiMg and inoculant used.

Other types of particles could be seen, mostly in frontier and in no-CHG areas such as (Ti,Mo,V,Nb)C carbides, where the predominant element is generally Ti. On a few occasions, apparently pure P, pure Sb or pure As could be observed. Also, some Ca-bearing precipitates (Ca-X) were sometimes noticed as already reported by Källbom [12]. Finally (Mg,Al,Si)N, SiO_2, FeSiMg and Mg_2Si precipitates were scarcely observed. It is noteworthy that the precipitates observed in the keel-blocks cast with melts doped in Si, Ce or inoculant are the same than those observed in heavy-section castings (trials PW-1, PW-2 and PW-3) made with usual melts. This confirms the possibility of studying CHG formation in light-section castings.

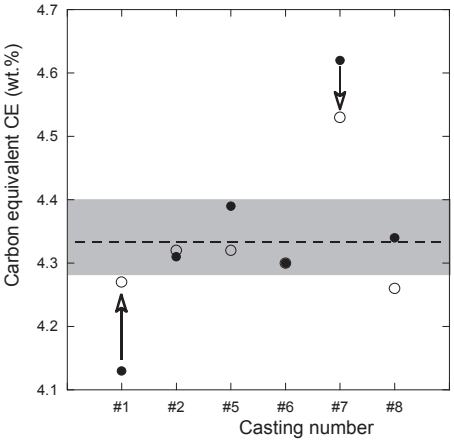

Fig. 3. Change of the CE values from the no-CHG (solid discs) to the CHG areas (open discs). The broken line stands for a eutectic CE (4.34 wt.%) and the greyed area shows the uncertainty on CE estimate.

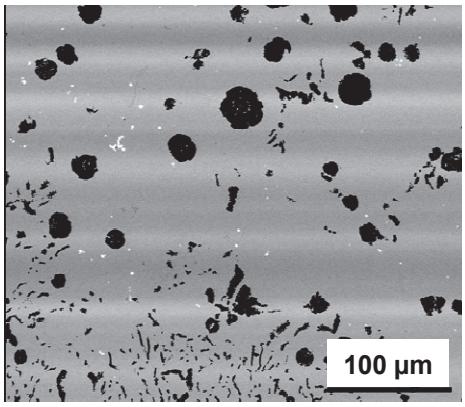

Fig. 4. Example of field for inclusion analysis showing a CHG area at the bottom and a frontier area at the top.

The amount of particles observed in CeMM-treated alloys is much higher than in those treated with Mg. This could possibly be related to the much stronger reaction during Mg-treatment that may favour entrapment of inclusions into the slag. On the other hand, no clear difference in the number of inclusions could be found among the three inspected areas for either of the investigated samples. However, there is less variation in the nature of the inclusions observed in the CHG areas that are mainly (Ce,La)S for CeMM treated irons and MgS for the FeSiMg ones, compared to the ones identified in the frontier and No-CHG areas, where other types of inclusions are found. This is certainly due to the fact that X-P and (Ti,M)C particles are usually found in the last solidified regions as a result of microsegregation.

As already mentioned by Källbom [12], oxygen-bearing particles were found essentially in areas out from the CHG cells suggesting a correlation between the low level of oxygen and CHG formation. Understanding this apparent contradiction that a spheroidizer such as Ce favours CHG formation while an element such as oxygen which is eliminated by the spheroidization treatment should be at a sufficient level to avoid CHG formation remains a challenge. Källbom [12] concluded to poor graphite nucleation kinetics because of the lack of available oxygen, but this contradicts recent results that showed increased inoculation leads to enhanced CHG formation [7, 10]. This suggests that the lack of oxygen affects graphite growth rather than its nucleation.

Conclusion

Ce addition to ductile iron castings promotes CHG formation under high cooling rates as it does in heavy-section parts. Ce was found to both decrease graphite nucleation and slow down graphite growth. Melts treated with Mg together with Ce did not show CHG except in the case of very high Si content. It has been observed that the composition of the CHG areas is near-eutectic both in hypo- and hyper-eutectic alloys cast in this work. This phenomenon could be designated as a meso-segregation, and indirectly confirms that CHG appearance is related to the eutectic reaction.

Over-treatment as performed in this work to enhance CHG formation in light-section castings led to precipitation of numerous inclusions that were found similar to those observed in usual castings. The number of inclusions is much higher in Ce-treated than in Mg-treated alloys, they are mainly (Ce,La)S and CeP in the former, MgS in the latter. Ti-rich carbides and P-rich compounds were hardly found in areas affected by CHG but located in the last to solidify zone and may thus be associated with microsegregation built-up at the end of the eutectic reaction. Oxygen-bearing inclusions were observed only out of the CHG cells as already reported.

Table 2. Summary of particles observations. When the number of particles was measured, average values per mm^{-2} are given, otherwise the observation is noted with ●.

Casting ref.	Treatment	Area	(Ce,La)S	MgS	CeP	(Ti,M)C	others
#5	CeMM	CHG	350		25		Ca-X
		frontier	255		250	15	MgO
#7	CeMM	CHG	400		120	28	
		Frontier	320		135	15	
		No-CHG	360		175	47	CeO, Ca-X
#11	CeMM	CHG	225		145	25	CeO, Ca-X
		No-CHG	430		90	8	CeO, Ca-X
#15	FeSiMg	CHG	40	130			(Mg,Al,Si)N, Ca-X
		Frontier	24	71		24	(Mg,Al,Si)N
		No-CHG	48	107	36	48	MgO, Ca-X
PW-1	FeSiMg	CHG	●	●	●	●	(Mg,Al,Si)N
		No-CHG	●	●	●	●	MgO, (Mg,Al,Si)N
PW-2	FeSiMg	CHG		●		●	Mg_2Si, (Mg,Al,Si)N
		Frontier	●	●	●	●	MgO
		No-CHG	●		●	●	Mg_2Si, MgO, CeO
PW-3	FeSiMg	CHG		36			MnS, Ca-X
		Frontier		190			(Mg,Al,Si)N, Ca-X
		No-CHG		60		60	MgO, MnO, (Mg,Al,Si)N, Ca-X
Ref. [12]	FeSiMg	CHG		●			Ca-X
		Frontier No-CHG					SiO_2

Acknowledgments

The authors would like to thank the financial support obtained from the Industry Department of the Spanish Government (ref. PROFIT FIT-030000-2007-94).

References

[1] S. I. Karsay: AFS Transactions Vol. 78 (1970), p. 85

[2] M. Gagné and D. Argo, in: Advanced Casting Technology, edited by J. Easwaren, ASM Int., Metals Park, OH (1987), p. 231

[3] A. Javaid and C. R. Loper Jr.: AFS Transactions Vol. 103 (1995), p. 135

[4] Z. Ignaszak: Materials Science (Medziagotyra) Vol. 9 (2003), p. 245

[5] R. Kallböm: Materials Science and Engineering A Vol. 413-414 (2005), p. 346

[6] M. Gagné and C. Labrecque: AFS Transactions Vol. 115 (2007), paper 07-004(05)

[7] I. Asenjo, P. Larrañaga, J. Sertucha, R. Suárez, J. M. Gómez, I. Ferrer and J. Lacaze: International Journal of Cast Metals Research Vol. 20 (2007), p. 319

[8] J. Sertucha, R. Suárez, I. Asenjo, P. Larrañaga, J. Lacaze, I. Ferrer and S. Armendariz: ISIJ International Vol. 49 (2009), p. 220

[9] P. Larrañaga, I. Asenjo, J. Sertucha, R. Suárez, I. Ferrer and J. Lacaze: Metallurgical and Materials Transactions Vol. 40A (2009), p. 654

[10] S. Méndez, P. Larrañaga, J. Izaga and R. Suárez: Proceedings 2010 World Foundry Congress, in press.

[11] S. Méndez, D. López, I. Asenjo, P. Larrañaga and J. Lacaze, unpublished research

[12] R. Källbom, K. Hamberg and L-E. Bjorkegren: World Foundry Congress (2006), paper 184